Pure Appl. Chem., Vol. 81, No. 2, pp. 263–272, 2009.
doi:10.1351/PAC-CON-08-08-16

Exploring RNA–ligand interactions*

Yitzhak Tor‡

Department of Chemistry and Biochemistry, University of California, San Diego, La Jolla, CA 92093, USA

Abstract: RNA molecules play essential roles in biological processes and are evolving as important targets for therapeutic intervention. Small molecules that specifically bind unique RNA sites and prevent the formation of functional RNA folds or RNA–protein complexes can modulate cell functions and can become of therapeutic potential. To explore such recognition events and to fabricate discovery assays, effective biophysical tools need to be advanced. When carefully designed, new fluorescent nucleosides can serve an unparalleled role in such studies. Our criteria for "ideal" fluorescent nucleoside analogs include: (a) high structural similarity to the native nucleobases to faithfully mimic their size and shape, as well as hybridization and recognition properties; (b) red-shifted absorption bands; (c) red-shifted emission band (preferably in the visible); (d) a reasonable emission quantum efficiency; and, importantly, (e) sensitivity of their photophysical parameters to changes in the microenvironment. Our program, aimed at the development of new emissive isomorphic nucleoside analogs, has yielded several useful nucleobases. Selected analogs were implemented in fluorescence-based assays. This overview presents the motivation for this work by introducing RNA–ligand interactions and discusses the design and synthesis of fluorescent isosteric nucleobase analogs and their utilization for the fabrication of "real-time" fluorescence-based biophysical assays.

Keywords: aminoglycoside antibiotics; fluorescence; fluorescent nucleosides; RNA.

RNA AS A TARGET

Key discoveries over the past few decades have cemented the role of RNA as a central biomolecule. No longer viewed as a passive carrier of genetic information, RNA is now recognized to constitute structurally and functionally sophisticated biopolymers, and to be involved in key cellular events. As such, RNA can be fundamentally viewed as a potential target for the control of cell function by exogenous ligands and for therapeutic intervention by drug-like small molecules [1]. Much like the development of low-molecular-weight ligands as modulators of protein function, one could envisage the discovery of small molecules as specific effectors of RNA structure and function and hence of cell fate [2]. With this goal in mind, we initiated, about 15 years ago, a research program that aimed at unraveling the fundamentals of RNA–ligand interactions and advancing RNA as a drug target [3].

Our search for small molecules as selective RNA binders was stimulated by the established ability of aminoglycoside antibiotics to interfere with ribosomal protein biosynthesis. Examples of these naturally occurring pseudo-oligosaccharides are shown in Fig. 1. The common core of most aminoglycosides is 2-deoxystreptamine (2-DOS), a highly functionalized amino-cyclitol. Functionalization of the 2-DOS core with additional aminosugars, typically at the 4- and 5-, or 4- and 6-positions, charac-

*Paper based on a presentation at the 17th International Conference on Organic Synthesis (ICOS 17), 22–27 June 2008, Daejeon, Korea. Other presentations are published in this issue, pp. 169–298.

‡E-mail: ytor@ucsd.edu

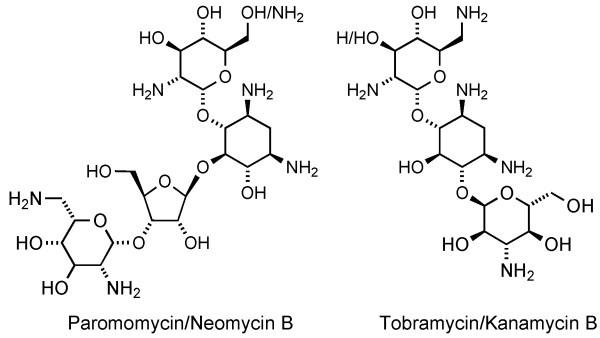

Fig. 1 Structures of aminoglycoside antibiotics that target ribosomal RNA.

terizes most aminoglycosides [4]. The abundance of protonable amino groups on these structures suggests a highly cationic character that may facilitate interactions with negatively charged biomolecules.

Several key discoveries highlighted aminoglycoside antibiotics as a family of RNA binders. In 1987, Noller identified specific binding sites for aminoglycosides on ribosomal RNA using footprinting techniques [5], substantiating an early proposal by Davies. In the early 1990s, Schroeder demonstrated that these antibiotics could also inhibit splicing of group I introns (a prototypical ribozyme) [6]. Further excitement was triggered by Green's 1993 report, demonstrating the capability of the same natural products to inhibit the interaction between the HIV-1 Rev protein and its cognate RNA target, the Rev response element [7]. These seminal papers, establishing aminoglycosides as RNA-selective binders, triggered numerous questions, including: (a) What is the role of electrostatic interactions in RNA–aminoglycoside binding? (b) How RNA-selective are these antibiotics? Do they bind other RNA targets? (c) Can multiple binding sites for aminoglycosides be found on RNA molecules? (d) Can a unified recognition model for RNA–aminoglycoside binding be formulated?

Years of investigations by our and other groups have ensued [3,8]. While the understanding of RNA–ligand recognition has significantly evolved over the past decade, the design and discovery of RNA-specific binders remained a nontrivial task. The major advancements and challenges include: (a) Most RNA folds do not possess deep solvent-excluded clefts. Numerous intermolecular contacts covering a significant surface area need to be established between the ligand and its RNA target to achieve adequate affinity and biologically relevant selectivity; (b) Electrostatic interactions play critical roles in many RNA–ligand complexes, creating a delicate interplay between overall charge, affinity, and selectivity. Highly charged ligands are likely to be promiscuous RNA binders; (c) RNA is a dynamic biomolecule and RNA–ligand binding generally involves conformational changes in both the RNA host and the incoming ligand (i.e., mutual induced-fit). Certain RNA targets are more flexible and forgiving than others. Furthermore, flexible small molecules can "remodel" according to the RNA topography and electrostatic potential, further complicating ligand design. These observations, together with pioneering molecular dynamics simulations by Hermann and Westhof [9], led to a proposed binding model that emphasizes a three-dimensional electrostatic complementarity between the aminoglycosides and their RNA hosts [10]; and, practically, (d) Limited availability of structure–activity relationships (SARs) challenges new ligand design.

To arrive at the observations summarized above, we have studied numerous RNA targets and examined their interactions with the natural antibiotics and systematically modified derivatives [3]. The following sections illustrate our early model system and its limitations, as well as the newer methods we have developed to facilitate the examination of RNA–ligand interactions and advance knowledge in this exciting field.

EXPLORING RNA–LIGAND INTERACTIONS

One of the most productive model systems we initially employed was the hammerhead (HH) ribozyme. This catalytic RNA is one of the best-characterized small RNA enzymes [11]. A wealth of information regarding its structural and biochemical features is available [12]. Of significance was the discovery that aminoglycosides inhibit the HH-mediated RNA cleavage reaction [13]. We therefore used this small RNA enzyme to assess the affinity of small molecules to RNA by simply following their ability to inhibit the ribozyme's activity [14]. In a typical experiment, the RNA substrate is radioactively labeled at its 5'-end. Upon annealing to the enzyme component, the cleavage reaction is initiated (Fig. 2). The reaction mixture is sampled and quenched at given time intervals. Polyacrylamide gel electrophoresis separates the cleaved product from the full-length RNA substrate, and the gel is quantified by phosphorimagery. This procedure is repeated in the presence of increasing concentrations of potential RNA inhibitors, and their potency is indirectly assessed based on their ability to inhibit the HH ribozyme cleavage.

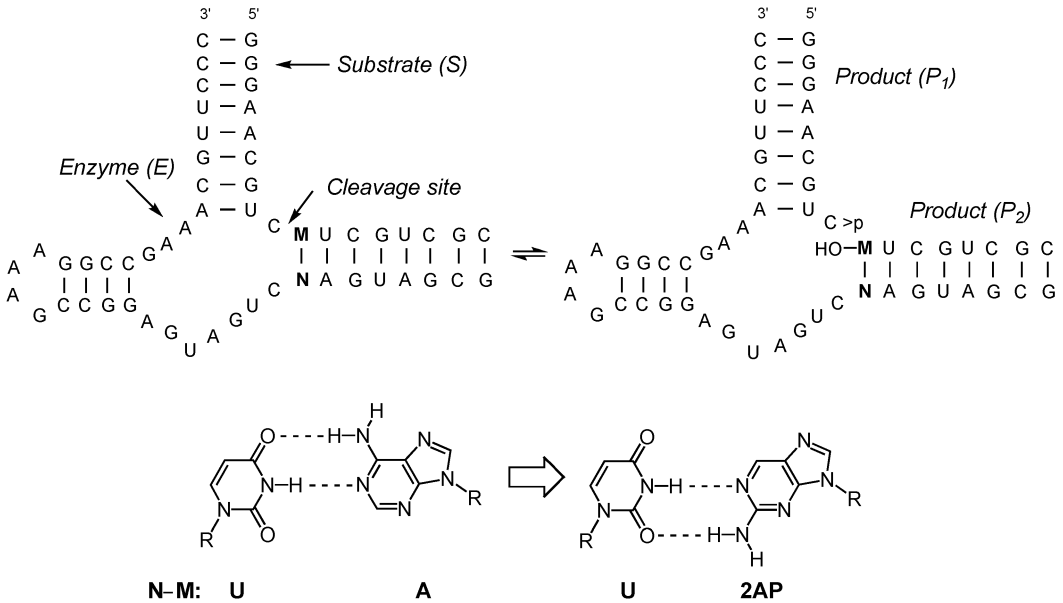

Fig. 2 (Top) HH ribozymes and the cleavage reaction. (Bottom) The isostructural U-A and U-2AP base pairs. In the fluorescent ribozyme, a U-2AP base pair replaces the natural U-A base pair [15].

While the method described above is sensitive and precise, it is exceedingly time-consuming. It is not conducive to high-throughput analysis of RNA binders and practically limits the number of experiments one can conduct. We therefore developed internally fluorescent HH ribozymes, such that enhancement of emission intensity directly reflects the progress of the ribozyme-mediated reaction in real time [15]. This was achieved by placing 2-aminopurine (2AP), an intensely fluorescent adenosine isoster, next to the site of cleavage (Fig. 2). Since 2AP's emission is highly sensitive to its environment, we anticipated that upon ribozyme-mediated cleavage of the substrate, 2AP would become exposed and its emission enhanced. This was experimentally validated and was employed to evaluate inhibitors potency under a variety of conditions [15]. In addition to providing a friendly, real-time tool for monitoring ribozyme catalysis and inhibition, internally fluorescent ribozymes provide prime examples for the tremendous utility of fluorescent nucleoside analogs [15].

FLUORESCENT NUCLEOSIDE ANALOGS: DESIGN AND SYNTHESIS

The demonstrated utility of 2AP and the scarcity of other useful emissive isosteric nucleoside analogs [16], have prompted us to initiate a new research program aimed at the design, synthesis, and implementation of new fluorescent nucleosides [17]. To be of utility, we have envisioned the new emissive nucleoside analogs to maintain the highest possible structural similarity to the natural nucleobases, to have their absorption and emission bands shifted to long wavelengths (>300 and >400 nm, respectively), to retain adequate emission quantum efficiencies and, importantly, to display sensitivity (of either λ_{em} and/or ϕ_F, τ) to their microenvironment.

Two primary scaffolds were initially explored (Fig. 3). The basic design principle has relied on conjugating or fusing five-membered aromatic heterocycles to the pyrimidine core. This has been inspired by the favorable photophysical properties of the parent conjugated heterocycles. For instance, 2-phenylfuran and benzofuran are much more emissive than their individual aromatic constituents [18,19]. This suggested to us that the analogous pyrimidine scaffolds should possess useful photophysical characteristics.

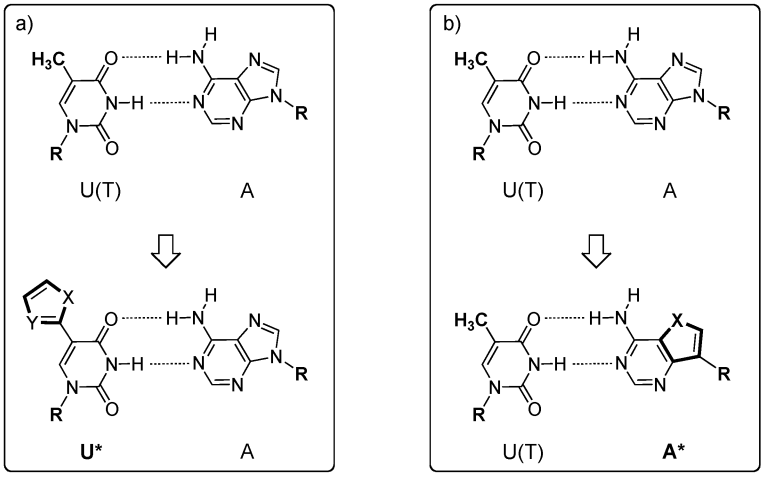

Fig. 3 Design of first-generation fluorescent nucleoside analogs: (a) emissive pyrimidines U*, and (b) emissive purines A* (X = O, S, Y = CH,N). Note, similar approaches apply for the analogous C and G analogs. R stands for D-ribose and 2'-deoxy-D-ribose.

The 5-modified pyrimidine analogs were synthesized using standard Stille coupling conditions, where the 2-tributylstannyl derivative was coupled to 5-iodo-2'-deoxyuridine (**1a**) or 5-iodo-uridine (**1b**) as illustrated in Scheme 1 for the furan analogs **2** and **3**, respectively [20,21]. To facilitate oligonucleotide synthesis, we regularly prepare both the phosphoramidite required for solid-phase oligonucleotide synthesis (e.g., **4**) as well as the corresponding triphosphate (e.g., **5**) that can be utilized for the enzymatic incorporation of the modified analog.

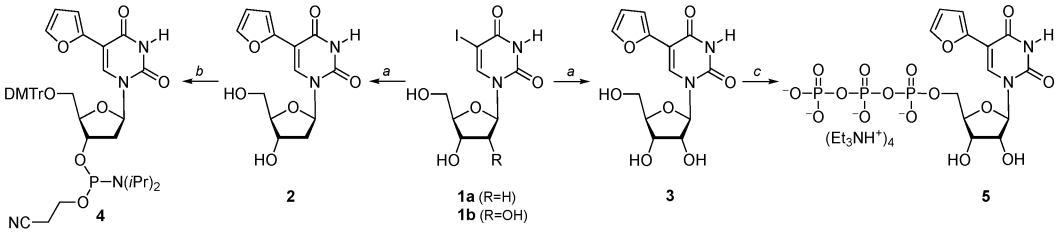

Scheme 1 Concise syntheses of 5-conjugated pyrimidines. *Typical reagents and conditions*: (a) 2-(tributylstannyl)furan, $PdCl_2(PPh_3)_2$, dioxane; (b) (i) DMTrCl, pyr, Et_3N, (ii) $(iPr_2N)_2POCH_2CH_2CN$, 1*H*-tetrazole, CH_3CN; (c) $POCl_3$, $(MeO)_3PO$, 0 °C; (ii) tributylammonium pyrophosphate, Bu_3N, 0 °C.

Scheme 2 illustrates the synthesis of a thieno[3,4-*d*]pyrimidine nucleoside analog **9**, as an example for an emissive fused pyrimidine [22]. The commercially available methyl 3-aminothiophene-4-carboxylate hydrochloride **6** was treated with KOCN to yield the corresponding urea **7**. Cyclization to the pyrimidine **8** was accomplished upon treatment with sodium methoxide in methanol. The emissive heterocycle **8** was then converted into the corresponding ribonucleoside **9** using a standard glycosylation procedure employing 1-*O*-acetyl-2,3,5-tri-*O*-Bz-ribofuranoside and trimethylsilyl trifluoromethanesulfonate (TMSOTf), followed by deprotection of all esters with aqueous ammonia [22]. To facilitate the incorporation of this modified ribonucleoside into oligonucleotides, both the triphosphate (**10**) and the (triisopropylsilyl)oxymethyl (TOM)-protected phosphoramidite were prepared.

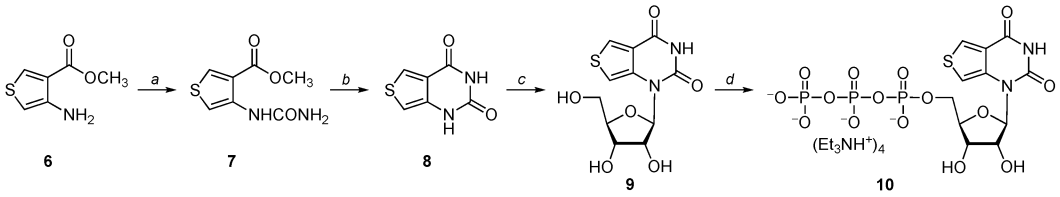

Scheme 2 Synthesis of thieno[3,4-*d*]pyrimidine-based nucleoside **9** and its triphosphate **10**. *Reagents and conditions*: (a) KOCN, aq. acetic acid, RT, 81 %; (b) NaOMe, MeOH, RT; (c) (i) *N*,*O*-bis(trimethylsilyl) acetamide, TMSOTf, CH_3CN, RT, 57 % (steps b and c); (ii) NH_4OH, dioxane, 60 °C, 84 %; (d) (i) $POCl_3$, $(MeO)_3PO$, 0–4 °C; (ii) tributylammonium pyrophosphate, Bu_3N, 0–4 °C, 56 %.

FLUORESCENT NUCLEOSIDE ANALOGS: PHOTOPHYSICAL PROPERTIES

To assess the potential of modified nucleosides as reporter nucleobases, we evaluate their photophysical properties and particularly the sensitivity of their absorption and emission spectra to changes in polarity [23]. While increasing solvent polarity has little influence on the absorption maxima of the modified ribonucleoside **3**, the emission maximum and intensity are significantly affected by solvent polarity (Fig. 4a) [21]. As solvent polarity is decreased from water to methanol, and finally acetonitrile, significant hypsochromic shift, and hypochromic effects are observed. In water, **3** exhibits a strong emission band with the maximum at 440 nm corresponding to more than 3-fold higher intensity relative to its emission in acetonitrile. Notably, an excellent correlation between emission energy and $E_T(30)$, a microscopic solvent polarity parameter [24], is seen (inset, Fig. 4a). A similar trend is observed for the fused thiophene-based nucleoside **9**, which emits at 412, 404, and 386 nm in water, methanol, and acetonitrile, respectively (Fig. 4b) [22]. As for **3**, excellent linear correlation between the emission energy of **9** and $E_T(30)$ is observed (inset, Fig. 4b).

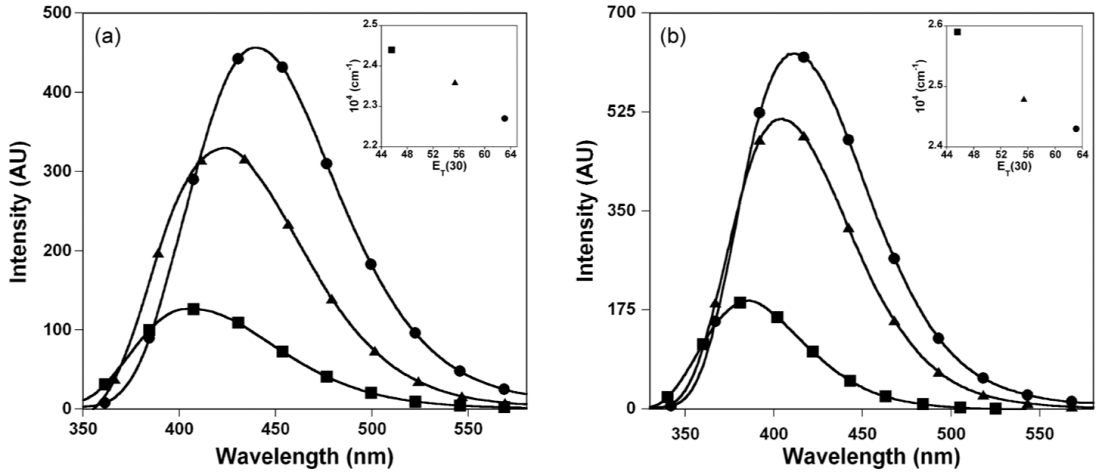

Fig. 4 (a) Emission spectra of nucleosides **3** (left) and **9** (right) in water (●), methanol (▲) and acetonitrile (■). *Insets:* Emission energy plotted against $E_T(30)$, a microscopic solvent polarity scale.

FLUORESCENT NUCLEOSIDE ANALOGS: APPLICATIONS

Antibiotics binding at the ribosomal A-site

To explore the utility of the furan-modified uridine **3** for the study of RNA–ligand interactions, we selected the bacterial decoding A-site as our first test system. This small internal loop within the 16S rRNA is the binding site of the naturally occurring aminoglycoside antibiotics, and has been extensively investigated as a target for the development of new antibiotics [1,25,26]. Studies have demonstrated that this site is an autonomous RNA domain capable of mimicking the function and antibiotics recognition features of the entire 16S rRNA [27]. This correlation has paved the way for the development of useful fluorescence-based assays for the discovery of A-site binders utilizing short RNA constructs [28,29]. In particular, aminoglycoside antibiotics interfere with the conformational flexibility of two adenine residues [30], A1492 and A1493 that are involved in mRNA decoding, a feature that is key to the 2AP-based fluorescence binding assays (Fig. 5). Recent structural investigations indicate that direct or water-bridged H-bonds to the neighboring G–C pairs and the noncanonical U1406•U1495 pair stabilize the A-site–aminoglycoside complexes [31], and prompt us to consider replacing one of the U residues with a fluorescent furan-containing analog **3** for generating a fluorescent reporting A-site construct (Fig. 5) [21].

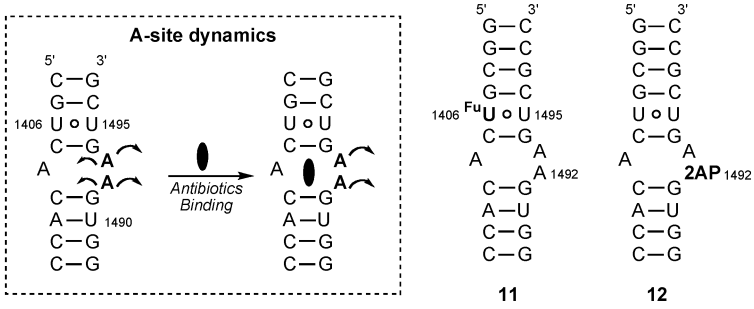

Fig. 5 The bacterial A-site, illustrating the dynamic residues within the aminoglycosides binding sites (framed). Also shown are two fluorescent A-site constructs, **11** and **12**, used to explore ligand binding.

When the A-site duplex construct **11**, containing a single emissive U analog **3** at position 1406, is excited at 322 nm and titrated with paromomycin, emission intensity at 433 nm steadily increases (Fig. 6). At saturation, nearly two-fold increase in emission intensity is observed, yielding an EC_{50} value of 11.5 ± 1 μM [21]. Binding of neomycin to the A-site duplex **11** was also signaled by enhanced fluorescence corresponding to an EC_{50} value of 5.0 ± 0.2 μM [21]. Interestingly, 2AP-modified duplex **12**, while responding well to increasing paromomycin concentrations, failed to show any significant response to neomycin [21].

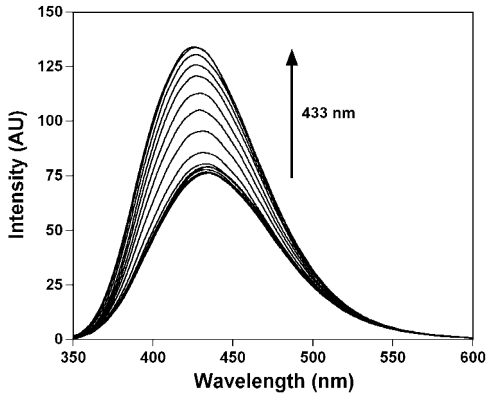

Fig. 6 Titration of duplex **11** with increasing concentrations of paromomycin in HEPES buffer (pH 7.4) containing 4.0 μM RNA. See ref. [21] for additional information.

Detecting the presence of abasic sites in RNA

The occurrence, significance, and repair of abasic sites in cellular RNA are largely unexplored [32]. Their appearance seems, however, to be almost exclusively associated with the activity of ribosome-inactivating proteins (RIPs), such as ricin and saporin. These plant toxins catalyze the depurination of a specific nucleotide within a conserved ribosomal RNA sequence known as the α-sarcin/ricin loop [33]. This deglycosylation reaction reduces the affinity of the ribosome to elongation factors that are critical for protein synthesis, resulting in disrupted protein production and ultimately cell death. To advance an effective method to detect RNA depurination by these toxic proteins, and to develop an effective assay for their activity and inhibition, we have sought new fluorescent nucleobase analogs that can positively respond to the presence of abasic sites in RNA.

We discovered that **9** (Scheme 2), a highly emissive pyrimidine analog (ϕ_F = 0.48), signals the presence of abasic RNA sites with significantly enhanced emission [34]. Studies were conducted with oligonucleotide **13** (Fig. 7) that was made using in vitro transcription reactions with triphosphate **10** (Scheme 2). As seen in Fig. 7, the short emissive oligonucleotide **13** displays significant emission quenching upon hybridization to perfect complements, as well as substantial fluorescence enhancement upon hybridization to complementary RNA and DNA oligonucleotides that contain an abasic site opposite the reporter nucleobase (Fig. 7). Notably, the probe reports the presence of an abasic site in an RNA–RNA duplex (**13•15**) with higher signal enhancement than the corresponding RNA–DNA duplex (**13•17**) [34]. This key observation inspired the development of the approach reported here for monitoring the depurination activity of RIPs using fluorescent RNA probes [34].

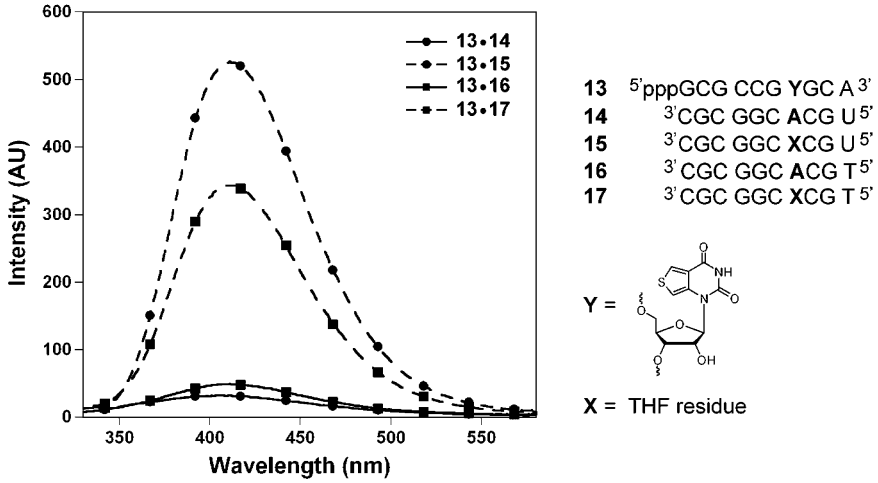

Fig. 7 Emission spectra of duplexes obtained upon hybridization of RNA **13** to its perfect RNA and DNA complements **14** and **16**, respectively, as well as to the corresponding abasic-containing constructs **15** and **17**, respectively. While both the perfect homo- and hetero-duplexes (**13•14** and **13•16**, respectively) are highly quenched, the duplexes containing a tetrahydrofuran (THF) residue (a stable abasic-site mimic) are highly emissive, with the RNA•RNA duplex **13•15** showing the highest intensity. Conditions: 1 μM duplex in 20 mM cacodylate buffer pH 7.0, 500 mM NaCl, 0.5 mM EDTA, 25 °C, λ_{ex} = 304 nm.

SUMMARY

Researchers have long relied on fluorescence-based techniques to decipher the fundamental structural, folding, and recognition features of biomolecules. Many proteins contain fluorescent aromatic amino acids (e.g., tryptophan), or interact with fluorescent cofactors (e.g., NADH), thus providing researchers with inherently emissive, "built-in", probes. Nucleic acids, in contrast, present challenges as the native nucleobases are practically non-emissive [35].

To advance the exploration of RNA–ligand interactions, we have embarked on a new project aimed at the expansion of the repertoire of useful fluorescent nucleosides available to the community. The results reported above validate our design principles, illustrating that emissive isomorphic nucleosides with favorable fluorescence properties can be attained using relatively minimal alterations of the natural nucleobases' structure.

From a fundamental physical organic chemistry perspective, predicting the emissive properties of small organic molecules based on their structure is, at this stage, impractical. One way to operate is to design structures by analogy to known chromophores. Even then, the ultimate test is empirical. This is particularly true for emissive nucleoside analogs, as their photophysical properties are further impacted when embedded within oligonucleotides, due to rigidification, de-solvation, and excited-state processes involving neighboring nucleotides. Even 2AP, one of the most commonly used isomorphic fluorescent nucleoside, does not always function optimally. This inherent challenge implies that universal approaches are unlikely to be found when fluorescence-based biophysical assays are concerned. Multiple fluorescent probes and constructs should be examined and optimized when a quest for effective fluorescence-based assays is initiated. Nevertheless, the future is bright and creative advances are likely to be embraced by bioorganic and biophysical chemists.

ACKNOWLEDGMENTS

I am grateful to the National Institutes of Health (grant numbers: AI 47673 and GM 069773) for support and my coworkers (particularly Dr. Seergazhi G. Srivatsan) for their insight and valuable contributions. I would also like to thank the organizers of ICOS-17 and Prof. Jaehoon Yu (Seoul National University) for their hospitality.

REFERENCES

1. T. Hermann, Y. Tor. *Exper. Opin. Therap. Patents* **15**, 49 (2005).
2. Y. Tor. *Angew. Chem., Int. Ed*. **38**, 1579 (1999).
3. (a) K. Michael, Y. Tor. *Chem.—Eur. J.* **4**, 2091 (1998); (b) Y. Tor. *ChemBioChem* **4**, 998, (2003); (c) Y. Tor. *Biochimie* **88**, 1045 (2006).
4. I. R. Hooper. In *Aminoglycosides Antibiotics. Handbook of Experimental Pharmacology*, S. Umezawa, I. R. Hooper (Eds.), Springer-Verlag, New York, **62**, 1 (1982).
5. D. Moazed, H. F. Noller. *Nature* **327**, 389, (1987).
6. U. von Ahsen, J. Davies, R. Schroeder. *Nature* **353**, 368 (1991).
7. M. L. Zapp, S. Stern, M. R. Green. *Cell* **74**, 969 (1993).
8. (a) T. Hermann. *Angew. Chem., Int. Ed.* **39**, 1890 (2000); (b) J. R. Thomas, P. J. Hergenrother. *Chem. Rev*. **108**, 1171 (2008).
9. T. Hermann, E. Westhof. *J. Mol. Biol.* **276**, 903 (1998).
10. Y. Tor, T. Hermann, E. Westhof. *Chem. Biol.* **5**, R277 (1998).
11. (a) O. C. Uhlenbeck. *Nature* **328**, 596 (1987); (b) K. R. Birikh, P. A. Heaton, F. Eckstein. *Eur. J. Biochem.* **245**, 1 (1997); (c) N. K. Vaish, A. R. Kore, F. Eckstein. *Nucleic Acids Res.* **26**, 5237 (1998).
12. (a) S. Verma, N. K. Vaish, F. Eckstein. *Curr. Opin. Chem. Biol.* **1**, 532 (1997); (b) J. E. Wedekind, D. B. McKay. *Annu. Rev. Biophys. Biomol. Struct.* **27**, 475 (1998); (c) T. K. Stage-Zimmermann, O. C. Uhlenbeck. *RNA* **4**, 875 (1998); (d) D. M. Zhou, K. Taira. *Chem. Rev*. **98**, 991 (1998); (e) M. Amarzguioui, H. Prydz. *Cell. Mol. Life Sci.* **54**, 1175 (1998).
13. T. K. Stage, K. J. Hertel, O. C. Uhlenbeck. *RNA* **1**, 95 (1995).
14. (a) H. Wang, Y. Tor. *J. Am. Chem. Soc.* **119**, 8734 (1997); (b) H. Wang, Y. Tor. *Bioorg. Med. Chem. Lett.* **7**, 1951 (1997); (c) H. Wang, T. Tor. *Angew. Chem., Int. Ed.* **37**, 109 (1998).
15. S. R. Kirk, N. W. Luedtke, Y. Tor. *Bioorg. Med. Chem*. **9**, 2295 (2001).
16. (a) M. E. Hawkins. *Cell Biochem. Biophys.* **34**, 257 (2001); (b) M. J. Rist, J. P. Marino. *Curr. Org. Chem.* **6**, 775 (2002); (c) A. Okamoto, Y. Saito, I. J. Saito. *Photochem. Photobiol. C: Photochem. Rev.* **6**, 108 (2005); (d) J. N. Wilson, E. T. Kool. *Org. Biomol. Chem*. **4**, 4265 (2006).
17. Y. Tor, S. Del Valle, D. Jaramillo, S. G. Srivatsan, A. Rios, H. Weizman. *Tetrahedron* **63**, 3608, (2007).
18. F. S. Wettack, R. Klapthor, A. Shedd, M. Koeppe, K. Janda, P. Dwyer, K. Stratton. *The Photophysics of Several Condensed Ring Heteroaromatic Compounds. NBS Special Publication (United States)*, **526**, 60 (1978).
19. N. J. Greco, Y. Tor. *Tetrahedron* **63**, 3515 (2007).
20. N. J. Greco, Y. Tor. *J. Am. Chem. Soc.* **127**, 10784 (2005).
21. S. G. Srivatsan, Y. Tor. *J. Am. Chem. Soc*. **129**, 2044 (2007).
22. S. G. Srivatsan, H. Weizman, Y. Tor. *Org. Biomol. Chem.* **6**, 1334 (2008).
23. R. W. Sinkeldam, Y. Tor. *Org. Biomol. Chem.* **5**, 2523 (2007).
24. C. Reichardt. *Chem. Rev.* **94**, 2319 (1994).
25. L. P. Kotra, J. Haddad, S. Mobashery. *Antimicrob. Agents Chemother.* **44**, 3249 (2000).
26. D. J. Knowles, N. Foloppe, N. B. Matassova, A. I. Murchie. *Curr. Opin. Pharmacol*. **2**, 501 (2002).

27. P. Purohit, S. Stern. *Nature* **370**, 659 (1994).
28. M. Kaul, C. M. Barbieri, D. S. Pilch. *J. Am. Chem. Soc*. **126**, 3447 (2004).
29. S. Shandrick, Q. Zhao, Q. Han, B. K. Ayida, M. Takahashi, G. C. Winters, K. B. Simonsen, D. Vourloumis, T. Hermann. *Angew. Chem., Int. Ed*. **43**, 3177 (2004).
30. M. Kaul, C. M. Barbieri, D. S. Pilch. *J. Am. Chem. Soc.* **128**, 1261 (2006).
31. B. Francois, R. J. M. Russell, J. B. Murray, F. Aboul-ela, B. Masquida, Q. Vicens, E. Westhof. *Nucleic Acids Res.* **33**, 5677 (2005).
32. (a) V. L. Schramm. *Curr. Opin. Chem. Biol.* **1**, 323 (1997); (b) P. A. Aas, M. Otterlei, P. O. Falnes, C. B. Vågbø, F. Skorpen, M. Akbari, O. Sundheim, M. Bjørås, G. Slupphaug, E. Seeberg, H. E. Krokan. *Nature* **421**, 859 (2003); (c) T. J. Begley, L. D. Samson. *Nature* **421**, 795 (2003); (d) J. D. Trzupek, T. L. Sheppard. *Org. Lett*. **7**, 1493 (2005); (e) P. A. Küpfer, C. J. Leumann. *ChemBioChem* **6**, 1970 (2005); (f) P. A. Küpfer, C. J. Leumann. *Nucleic Acids Res.* **35**, 58 (2007).
33. (a) Y. Endo, I. G. Wool. *J. Biol. Chem*. **257**, 9054 (1982); (b) R. R. Gutell, M. W. Gray, M. N. Schnare. *Nucleic Acids Res.* **21**, 3055 (1993); (c) K. Nielsen, R. S. Boston. *Annu. Rev. Plant Physiol. Plant Mol. Biol.* **52**, 785 (2001).
34. S. G. Srivatsan, N. J. Greco, Y. Tor. *Angew. Chem., Int. Ed.* **47**, 6661 (2008).
35. Y. Tor. *Tetrahedron* **63**, 3425 (2007).